New Classes of Magnetic Noise Self-Compensation Effects in Atomic Comagnetometer

Yushu Qin,* Zhenhan Shao,* Taizhou Hong, Yuanhong Wang, Min Jiang,† and Xinhua Peng‡
CAS Key Laboratory of Microscale Magnetic Resonance and School of Physical Sciences, University of Science and Technology of China, Hefei 230026, China;
CAS Center for Excellence in Quantum Information and Quantum Physics, University of Science and Technology of China, Hefei 230026, China
and Hefei National Laboratory, University of Science and Technology of China, Hefei 230088, China

(Received 22 January 2024; accepted 6 June 2024; published 11 July 2024)

Precision measurements of anomalous spin-dependent interactions are often hindered by magnetic noise and other magnetic systematic effects. Atomic comagnetometers use the distinct spin precession of two species and have emerged as important tools for effectively mitigating the magnetic noise. Nevertheless, the operation of existing comagnetometers is limited to very low-frequency noise commonly below 1 Hz. Here, we report a new type of atomic comagnetometer based on a magnetic noise self-compensation mechanism originating from the destructive interference between alkali-metal and noble-gas spins. Our comagnetometer employing K-^{3}He system remarkably suppresses magnetic noise exceeding 2 orders of magnitude at higher frequencies up to 160 Hz. Moreover, we discover that the capability of our comagnetometer to suppress magnetic noise is spatially dependent on the orientation of the noise and can be conveniently controlled by adjusting the applied bias magnetic field. Our findings open up new possibilities for precision measurements, including enhancing the search sensitivity of spin-dark matter particles interactions into unexplored parameter space.

DOI: 10.1103/PhysRevLett.133.023202

Anomalous spin-dependent interactions, which go beyond the standard model of particle physics, have garnered significant interest within the precision measurement community over the past decade [1,2]. These anomalous interactions encompass searches for spin-dark matter particles interactions [3–10], exotic spin-dependent forces [11–17], permanent electric dipole moments [18–21], spin-gravity coupling [22–26], as well as tests of *CPT* and Lorentz invariance [27–29], which could generate pseudomagnetic fields on nuclear spins, such as ^{3}He and ^{129}Xe. However, these experiments frequently encounter limitations imposed by magnetic noise and other systematic effects related to normal magnetic fields [30–33]. To overcome these challenges, atomic comagnetometers provide a crucial solution, which employs the distinct spin precession of two species to mitigate the effects of magnetic field drift and fluctuations but remains sensitive to pseudomagnetic fields [30,34].

Atomic comagnetometers can be implemented in various configurations. For example, noble-gas comagnetometers using ^{3}He-^{129}Xe [33,35] and ^{129}Xe-^{131}Xe [11,15,25,36], mercury comagnetometers using a ^{199}Hg-^{201}Hg pair [17,22], and alkali-metal comagnetometers [26,37], have been employed to suppress long-term drift in the axial magnetic field. Alkali-noble-gas comagnetometers, such as those based on K-^{3}He [9,10,38] and K-Rb-^{21}Ne pairs [28,39–41], operate at near-dc frequencies commonly below 1 Hz. Additionally, several comagnetometers based on certain molecular systems have also been developed for this purpose [6,23,24]. However, the exploration and demonstration of comagnetometers for the suppression of magnetic noise are still limited to low-frequency noise, hindering the investigation of spin-dependent interactions across a vast unexplored parameter space. For example, recent theoretical motivations in exploration of the interaction between spin and axion dark matter require the extension of measurement frequencies to values significantly higher than 1 Hz [1,2].

In this Letter, we report a new type of atomic comagnetometer based on magnetic noise self-compensation effects. These effects arise from the destructive interference between alkali-metal and noble-gas spins induced by their spin-exchange coupling. The coupling results in a mutual influence on the spin behavior of both species, rendering them interdependent. Consequently, the noble-gas response to magnetic noise, transmitted to alkali-metal spins through spin-exchange coupling as an effective magnetic field, interferes with the response of alkali-metal spins to magnetic noise. Under appropriate experimental conditions, this interference can be destructive, leading to significant self-compensation of magnetic noise. We demonstrate this mechanism in experiment using the K-^{3}He system, achieving a remarkable suppression of magnetic noise by at least 2 orders of magnitude. Unlike existing comagnetometers that suppress near-dc magnetic noise [15,16,22–26,35–39], our work realizes magnetic noise self-compensation at

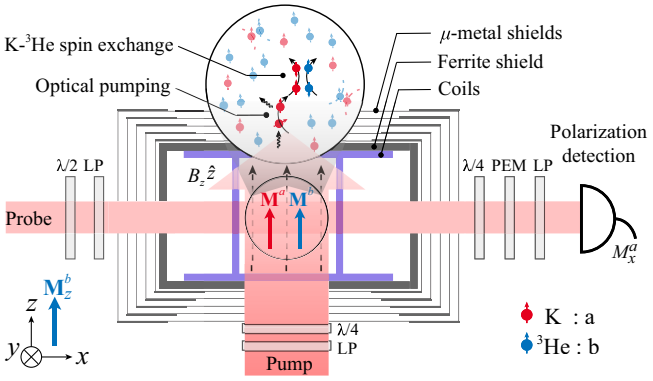

FIG. 1. Schematic of magnetic noise self-compensation experiment. Alkali-metal and noble-gas atoms are initially polarized along z. Alkali spins are probed along x. The spin-exchange coupling leads to an effective field experienced by alkali spins. The noble-gas response to magnetic noise interferes with the alkali-metal response via the effective field. The magnetic noise is self-compensated when such interference is destructive. LP, linearly polarizer; $\lambda/4$, quarter-wave plate; PEM, photoelastic modulator.

higher frequencies up to 160 Hz. We also observe that the capability of noise suppression depends on the direction of magnetic noise and can be conveniently controlled by adjusting bias magnetic field. We develop a comprehensive theory to explain these magnetic noise self-compensation effects, notable for its capacity to suppress normal magnetic noise while maintaining sensitivity to pseudomagnetic fields, holding the potential applications in searches for various anomalous spin-dependent interactions [5–15].

Our investigation into magnetic noise self-compensation employs an overlapping spin ensemble comprising potassium and ^{3}He gases. The experimental setup and spin dynamics are shown schematically in Fig. 1. A spherical GE180 glass cell with a diameter of 2 cm encloses a droplet of K, 2.5 amagat of ^{3}He and 200 torr of nitrogen. The ^{3}He nuclear spins are polarized along z via spin-exchange collisions with optically pumped K atoms [42–44]. The frequent spin-exchange collisions between K and ^{3}He result in an effective magnetic field $\lambda\mathbf{M}^a$ experienced by ^{3}He due to K and $\lambda\mathbf{M}^b$ experienced by K due to ^{3}He [38,45]. Here, "a" denotes alkali metal and "b" denotes noble gas. The direction of the projection of $\lambda\mathbf{M}^b$ along z (λM_z^b) is defined as the positive z axis. The bias field B_z is along z. It is defined as positive when it is consistent with the direction of λM_z^b, otherwise it is negative. Both species of spins precess around the sum of the applied bias field and their respective effective fields. In the linearization approximation, we express the evolution of the complex transverse magnetization $M_+^{a,b} = M_x^{a,b} + iM_y^{a,b}$ using a matrix representation [44]:

$$\partial_t \begin{pmatrix} M_+^a \\ M_+^b \end{pmatrix} = \begin{pmatrix} i\omega_a - \Gamma_a & -i\gamma_a \lambda M_z^a \\ -i\gamma_b \lambda M_z^b & i\omega_b - \Gamma_b \end{pmatrix} \begin{pmatrix} M_+^a \\ M_+^b \end{pmatrix} - iB_+ \begin{pmatrix} \gamma_a M_z^a \\ \gamma_b M_z^b \end{pmatrix}, \tag{1}$$

where $\omega_a = \gamma_a(B_z + \lambda M_z^b)$ and $\omega_b = \gamma_b(B_z + \lambda M_z^a)$ denote the Larmor frequencies of K and ^{3}He, respectively. Here, $\gamma_{a,b}$ and $\Gamma_{a,b}$ are the gyromagnetic ratios and decoherence rates of K and ^{3}He, respectively; $\lambda = 8\pi\kappa_0/3$ with the Fermi-contact enhancement factor $\kappa_0 \approx 5.9$ for K and ^{3}He [42]. The nondiagonal elements signify the spin-exchange coupling between these two spin species. Additionally, the last term accounts for the perturbation introduced by the complex ambient noise field $B_+ = B_x + iB_y$ in the xy plane. This noise field acts simultaneously on both spins. In the case of an oscillating magnetic noise, $B_+ = Be^{i\theta}\cos\omega t$, where θ is the azimuth angle characterizing the orientation of the noise field relative to the $+x$ axis. The magnetic response of our comagnetometer is measured by optically detecting the K magnetization along x (i.e., M_x^a) with a linearly polarized laser (Fig. 1) [44].

The magnetic self-compensation mechanism of the comagnetometer is essentially the destructive interference of two species. According to Eq. (1), the interference arises between ^{3}He response to magnetic noise, which is transmitted to K spins via the effective field λM_+^b, and K response to magnetic noise. By carefully selecting appropriate values for experimental parameters, such as B_z, λM_z^a, λM_z^b, the interference can be made destructive, resulting in the emergence of magnetic noise self-compensation of the measured K response M_x^a.

Figure 2 shows the magnetic response of our comagnetometer at various oscillation frequencies. During the experiment, the effective field of noble gas λM_z^b is adjusted to approximately 120 nT, which is achieved by changing the vapor-cell temperature and thus controlling the degree of polarization of ^{3}He. We apply a transverse magnetic field along the azimuth angle $\theta = \theta_{sc}$ (see below) as a test field, scan its frequency from 1–25 Hz, and record the corresponding response. When $B_z \approx -323$ nT, the comagnetometer response is suppressed by a factor of $\eta \approx 286$ in the vicinity of 8.3 Hz [Fig. 2(a)], compared with the individual K response which is calibrated using a signal deviating from the ^{3}He Larmor frequency and used as a normalized amplitude [44]. The frequency where the response is significantly suppressed is referred to as the "self-compensation frequency" and denoted by ω_{sc}, e.g., $\omega_{sc}/2\pi \approx 8.3$ Hz in Fig. 2(a). When $B_z \approx 323$ nT, the response is suppressed by a factor of about 582 around $\omega_{sc}/2\pi \approx 12.2$ Hz [Fig. 2(b)]. We also observe an enhancement at the ^{3}He Larmor frequency $|\omega_b|/2\pi \approx 10.5$ Hz (away from $\omega_{sc}/2\pi$), corresponding to the large peaks in Figs. 2(a) and 2(b). As detailed in Supplemental Material [44], our comagnetometer response can be well described by a Fano profile [46] defined as

$$A(\omega) \approx A_0(\omega)\left[\frac{(q+\varepsilon)^2}{1+\varepsilon^2}\right]^{1/2}, \tag{2}$$

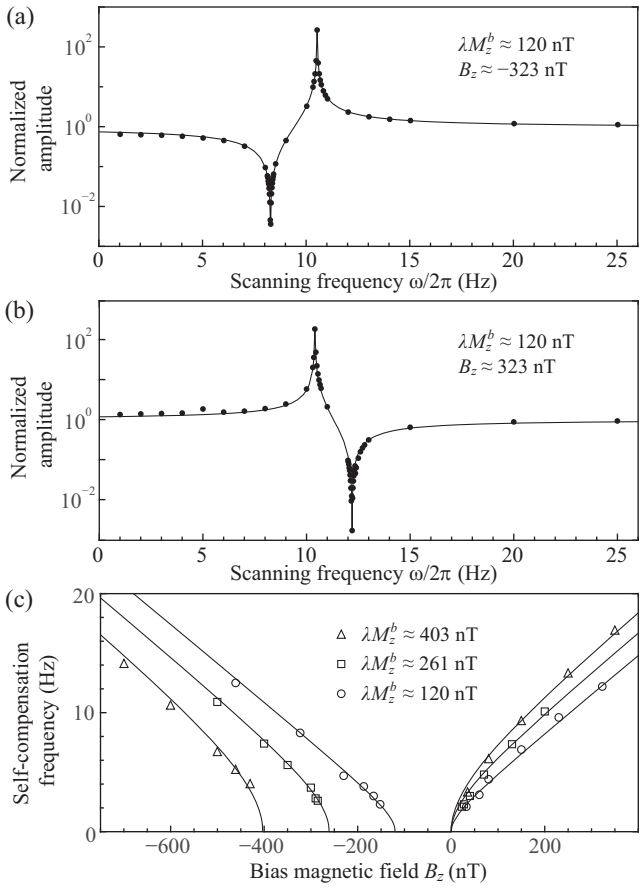

FIG. 2. Demonstration of self-compensation effect. (a),(b) Responses and corresponding Fano profile fits under a negative or positive bias field as a function of the oscillation frequency ω of the test field B_+. Both responses are suppressed by over 2 orders of magnitude near the self-compensation frequency. Each magnetic response is measured at its own self-compensation angle θ_{sc} of 163° and 36°, respectively (as discussed below). (c) Self-compensation frequencies as a function of B_z. Each curve consists of two branches corresponding to negative and positive B_z, respectively.

where $\varepsilon = (\omega - |\omega_b|)/\Gamma_b$ varies with the scanning frequency ω and q denotes Fano parameter that satisfies $(q\Gamma_b - |\omega_b|)^2 = \gamma_b^2 B_z(B_z + \lambda M_z^b)$ [44].

Here, $A_0(\omega)$ represents the individual K response to the oscillating field and the second factor $[(q+\varepsilon)^2/(1+\varepsilon^2)]^{1/2}$ only depends on noble gas. We surprisingly find that the total response $A(\omega)$ of the K-^{3}He comagnetometer is the product of these two terms. As shown in Eq. (2), when $q + \varepsilon \approx 0$ is satisfied, the destructive interference occurs and the response $A(\omega)$ is minimal. Under this condition, our comagnetometer can automatically self-compensate magnetic noise whose amplitude satisfies the linearization approximation [44], regardless of their unknown magnitudes. Consequently, we obtain the frequency where the response is minimized, corresponding to the aforementioned self-compensation frequency ω_{sc} [44],

$$\omega_{sc} \approx \gamma_b \left[B_z\left(B_z + \lambda M_z^b\right)\right]^{1/2}. \tag{3}$$

Additionally, the response-enhanced frequency corresponds to $\varepsilon = 0$, i.e., $\omega = |\omega_b|$ [see the peaks in Figs. 2(a) and 2(b)]. This enhanced effect has been studied in our recent works [7,12,13], which is outside the scope of this work.

The self-compensation frequency ω_{sc} can be controlled by adjusting the bias field B_z. Figure 2(c) illustrates the measured ω_{sc} as a function of B_z, which agrees well with the corresponding theoretical curves obtained from Eq. (3). Each curve, for a specific value of λM_z^b, consists of two branches separated by a gap. Taking the case of $\lambda M_z^b \approx 120$ nT as an example, when $|B_z| \gg 120$ nT (e.g., $B_z \approx \pm 323$ nT), a linear relationship between ω_{sc} and B_z is observed. This linearity can be seen from the simplified form of Eq. (3): $\omega_{sc} \approx |\omega_b| + (B_z/|B_z|)\gamma_b \lambda M_z^b/2$ when $|B_z|$ significantly exceeds λM_z^b. Negative values of B_z correspond to the left branch, where ω_{sc} is lower than the Larmor frequency of ^{3}He [e.g., see Fig. 2(a)], while positive values of B_z correspond to the right branch, where ω_{sc} is higher than the Larmor frequency of ^{3}He [e.g., see Fig. 2(b)]. When B_z approaches 0 or $-\lambda M_z^b$, the dependence between ω_{sc} and B_z becomes nonlinear. It is noteworthy that when B_z is tuned to approximately cancel the ^{3}He effective field (i.e., $B_z \approx -\lambda M_z^b$), our comagnetometer operates similarly to existing comagnetometers [38,39] that only suppress near-dc magnetic noise. In the range of -120 nT $< B_z < 0$, ω_{sc} becomes purely imaginary according to Eq. (3), lacking physical significance. By taking the real part of ω_{sc}, we obtain $\mathrm{Re}(\omega_{sc}) = 0$ Hz, at which the noise is expected to be mostly suppressed. This expected phenomenon is confirmed in our experiment. By adjusting B_z, our comagnetometer can accomplish an extended frequency range for suppressing magnetic noise, encompassing frequencies from near-dc to high frequency, for example, 160 Hz. Similar patterns are observed under varying λM_z^b and we present three measured curves with different λM_z^b by adjusting the vapor cell temperature. Here, λM_z^b is calibrated by applying a magnetic pulse along y and measuring the K Larmor frequency ω_a [44].

We demonstrate that the capability of suppressing magnetic noise depends on the azimuth angle θ of the field. This is due to the fact that the measured quantity in experiments, denoted as M_x^a, can be influenced by both the rotating and counterrotating components of the oscillating field. When the frequency of the oscillating noise field matches the self-compensation frequency ω_{sc}, these two components contribute equally in magnitude but with a phase difference of about $\pi + 2(\theta - \mathrm{arccot}\omega_a/\Gamma_a)$ [44]. To compensate for this phase difference, we can adjust the azimuth angle to

$$\theta_{sc} \approx \mathrm{arccot}\left[\gamma_a\left(B_z + \lambda M_z^b\right)/\Gamma_a\right], \tag{4}$$

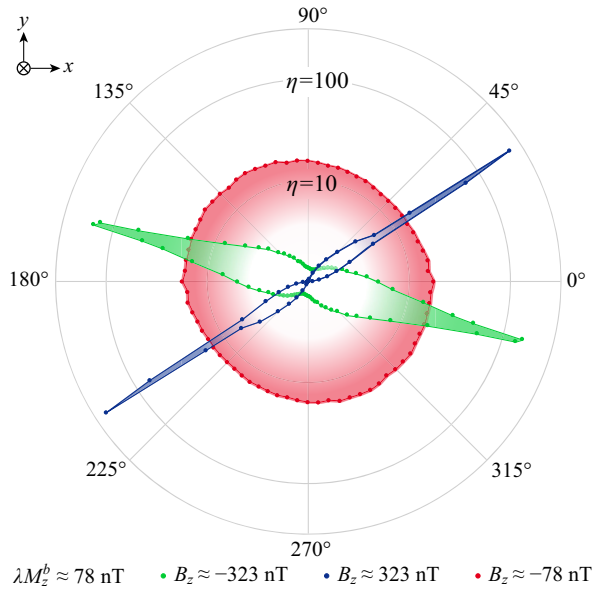

FIG. 3. Spatial dependence of the self-compensation effect. The suppression factors η are measured in different transverse directions and plotted as radial coordinates in a polar diagram, where the numbers 10 and 100 on the circles indicate the magnitude of the respective suppression factors. When $B_z \approx -323$ nT, 323 nT is applied, the suppression factor η is over 2 orders of magnitude near the angle of 165° and 32°, respectively. The noise suppression is over one order of magnitude in all transverse directions with $B_z \approx -\lambda M_z^b \approx -78$ nT, the same with existing self-compensated comagnetometers which suppress near-dc magnetic noise.

which is referred to as self-compensation angle, and the comagnetometer can achieve maximal suppression by canceling out the two components. Specifically, we set the bias field at approximately $B_z \approx -323$ nT as an example. This bias field corresponds to the theoretical self-compensation angle of $\theta_{sc} \approx 169°$ calculated using measured alkali-metal relaxation rate $\Gamma_a \approx 2$ kHz. We perform experiments to validate our theory. For an applied test field in a certain direction, we can obtain the suppression factor η by measuring the response at the self-compensation frequency ω_{sc}. Then we scan the test field angles to optimize and obtain the angle θ_{sc} with the largest suppression factor. As shown in Fig. 3 (the green curve), the self-compensation angle maximizing the noise suppression is about $\theta_{sc} \approx 165°$, which closely aligns with the theoretical prediction. Similarly, we adjust the bias field to 323 nT (the blue curve) and observe that the self-compensation angle moves to $\theta_{sc} \approx 32°$ in experiment. In these examples, the noise suppression exceeds 2 orders of magnitude.

We find that the noise suppression is independent of the azimuth angle θ when the bias field is set to be nearly equal in magnitude but opposite in direction to the ^{3}He effective field. As an example in our experiment, we set the bias field $B_z \approx -\lambda M_z^b \approx -78$ nT. In this case, the comagnetometer is capable of suppressing slowly fluctuating magnetic noise. We thus apply an oscillating transverse field as a test field with a frequency of 0.1 Hz. We find that regardless of the chosen angle θ, a suppression of at least one order of magnitude can be achieved (see the red curve of Fig. 3), which is the same situation as that shown in Fig. 2(c) with $B_z \approx -\lambda M_z^b$ where our comagnetometer operates similarly to existing comagnetometers which suppress near-dc magnetic noise. This occurs because the near-dc components of both the rotating field and the counterrotating field approach zero, irrespective of the phase compensation associated with the azimuth angle [44]. While the comagnetometer operating at $B_z \approx -\lambda M_z^b$ exhibits superior spatial-independence performance compared with other conditions, it is mainly suitable for suppressing magnetic noise at near-dc frequencies. However, a significant number of measurements of interest fall within higher frequencies. Consequently, it is important to extend the capability of spatially independent magnetic noise self-compensation to higher frequencies. One potential solution to address this challenge is the use of quadrature detection [44,47]. By employing quadrature detection where one can use two lasers along x and y as two probes, we measure both M_x^a and M_y^a simultaneously, instead of solely focusing on M_x^a. These measurements can then be combined to form $M_+^a = M_x^a + iM_y^a$. Further details, regarding how the response M_+^a remains unaffected by the azimuth angle of the magnetic noise are available in Supplemental Material [44].

We would like to emphasize the main differences between our work and previous studies. Existing atomic comagnetometers, such as those utilizing ^{129}Xe-^{131}Xe [11,15,25,36] and ^{3}He-^{129}Xe pairs [33,35], detect the free precession of the two spin species. The distinct precession frequencies are differentially processed to reduce axial magnetic noise within the dc and extremely low-frequency range, typically below 0.1 Hz. Another type of existing comagnetometers is alkali-noble-gas comagnetometers, such as those employing K-^{3}He and K-Rb-^{21}Ne pairs [39,40], operating under a specific bias field $B_z \approx -\lambda M_z^b$. They were first reported in the pioneering work [38] and referred to as "self-compensated comagnetometers." These comagnetometers can mitigate the slowly fluctuating magnetic noise commonly below 1 Hz [38,39]. However, for noise at higher frequencies, the effectiveness of previous magnetic noise self-compensation techniques deteriorates [30]. In contrast, our research unveils a new class of magnetic noise self-compensation effects that extend the efficacy of noise suppression to the high-frequency range, which differ from previous studies in physical mechanisms and operation conditions (see Supplemental Material [44]). First, previous self-compensated comagnetometers employ the adiabatic elimination of the near-dc changes in external fields, while our comagnetometer is based on the destructive interference between the two spin species even for high-frequency noise. Second, the previous

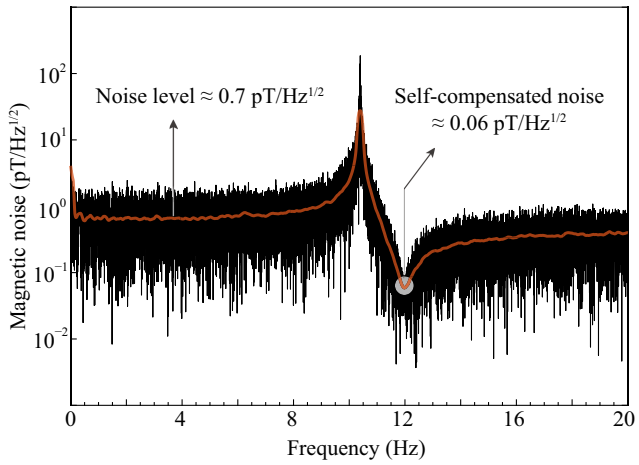

FIG. 4. White magnetic noise self-compensation. A wide-spectrum white noise of about 0.7 $\mathrm{pT}/\mathrm{Hz}^{1/2}$ is applied to simulate the shield Johnson noise. The noise is suppressed to around 0.06 $\mathrm{pT}/\mathrm{Hz}^{1/2}$ by over one order of magnitude near $\omega_{\mathrm{sc}}/2\pi \approx 12$ Hz.

self-compensation condition is removed in our work and the bias field B_z can be adjusted away from $-\lambda M_z^b$. Consequently, according to Eq. (3), the self-compensation frequency ω_{sc} can also be manipulated across a much broader range than before, spanning from 1–160 Hz.

Our findings would contribute to overcoming the magnetic noise limit in a series of spin-dependent physics experiments including searching for dark matter and exotic spin-dependent forces within the frequency range of near-dc to, for instance, 160 Hz [3–11,15–17,39]. As predicted by numerous theories beyond the standard model of particle physics, dark matter particles such as ultralight axions and axionlike particles couple with nuclear spins and behave as pseudomagnetic fields with oscillation frequencies equal to the Compton frequencies of these hypothetical particles [3–6,48]. The frequency range of near-dc to 160 Hz corresponds to dark matter masses up to pico-electron-volt level. Similarly, effects of exotic spin-dependent forces on nuclear spins are also equivalent to oscillating magnetic fields [11–15,49,50]. Particularly, there is a class of spin-dependent forces, i.e., velocity-dependent interactions, whose higher modulation frequencies lead to larger pseudomagnetic signals [12,14,49,50]. These pseudomagnetic fields do not affect alkali-metal spins and, therefore, are not self-compensated (see Supplemental Material [44] for details). Therefore, the comagnetometers remain sensitive to these pseudomagnetic fields.

The sensitivity of pseudomagnetic measurements, often limited by white Johnson noise from magnetic shields like μ metal and ferrite [31,32,39], necessitating improvement. The noise levels in these materials range from below 1 to 10 $\mathrm{fT}/\mathrm{Hz}^{1/2}$ [51]. Superconducting shields, free of thermal noise in principle, still face sensitivity limits around 1 $\mathrm{fT}/\mathrm{Hz}^{1/2}$ due to usage of thermal radiation shields [52]. Gradiometer arrangements [31,32], which reduce thermal shield noise by subtracting outputs from closely aligned detectors, inadvertently eliminate the pseudomagnetic fields of interest, making them unsuitable for these measurements. Despite these challenges, the high-frequency self-compensation method introduced here shows promise in enhancing pseudomagnetic detection sensitivity. Although our experiment has not yet reached the thermal shield noise limit, various works have been progressively approaching it [39]. To assess our comagnetometer's performance in suppressing such Johnson noise in advance, we apply a 0.7 $\mathrm{pT}/\mathrm{Hz}^{1/2}$ Gaussian white noise and observe the noise suppression by over one order of magnitude near $\omega_{\mathrm{sc}}/2\pi \approx 12$ Hz, as shown in Fig. 4. Importantly, this suppression technique remains effective against real thermal shield noise, potentially enhancing pseudomagnetic detection sensitivity to around 0.1 $\mathrm{fT}/\mathrm{Hz}^{1/2}$ over an extended frequency range.

In conclusion, our work has reported a new class of magnetic noise self-compensation effects and demonstrated an atomic comagnetometer expanding the capabilities of existing comagnetometers to higher frequencies. Although initially demonstrated with K-^{3}He system, this self-compensation mechanism should be applicable to a wide range of alkali-noble-gas systems, potentially propelling various researches on anomalous spin-dependent interactions [3,7,8,14,15].

This work was supported by the Innovation Program for Quantum Science and Technology (Grant No. 2021ZD0303205), National Natural Science Foundation of China (Grants No. T2388102, No. 11927811, No. 12150014, No. 12274395, No. 12261160569), and Youth Innovation Promotion Association (Grant No. 2023474). Chinese Academy of Sciences Magnetic Resonance Technology Alliance Research Instrument and Equipment Development/Functional Development (Grant No. 2022GZL003).

*These authors contributed equally to this letter.
†Contact author: dxjm@ustc.edu.cn
‡Contact author: xhpeng@ustc.edu.cn

[1] M. Safronova, D. Budker, D. DeMille, D. F. Jackson Kimball, A. Derevianko, and C. W. Clark, Search for new physics with atoms and molecules, Rev. Mod. Phys. **90**, 025008 (2018).
[2] D. DeMille, J. M. Doyle, and A. O. Sushkov, Probing the frontiers of particle physics with tabletop-scale experiments, Science **357**, 990 (2017).
[3] D. Budker, P. W. Graham, M. Ledbetter, S. Rajendran, and A. O. Sushkov, Proposal for a cosmic axion spin precession experiment (CASPEr), Phys. Rev. X **4**, 021030 (2014).

[4] C. Smorra *et al.*, Direct limits on the interaction of antiprotons with axion-like dark matter, Nature (London) **575**, 310 (2019).

[5] A. Garcon *et al.*, Constraints on bosonic dark matter from ultralow-field nuclear magnetic resonance, Sci. Adv. **5**, eaax4539 (2019).

[6] T. Wu *et al.*, Search for axionlike dark matter with a liquid-state nuclear spin comagnetometer, Phys. Rev. Lett. **122**, 191302 (2019).

[7] M. Jiang, H. Su, A. Garcon, X. Peng, and D. Budker, Search for axion-like dark matter with spin-based amplifiers, Nat. Phys. **17**, 1402 (2021).

[8] C. Abel *et al.*, Search for axionlike dark matter through nuclear spin precession in electric and magnetic fields, Phys. Rev. X **7**, 041034 (2017).

[9] J. Lee, M. Lisanti, W. A. Terrano, and M. Romalis, Laboratory constraints on the neutron-spin coupling of feV-scale axions, Phys. Rev. X **13**, 011050 (2023).

[10] I. M. Bloch, R. Shaham, Y. Hochberg, E. Kuflik, T. Volansky, and O. Katz, Constraints on axion-like dark matter from a serf comagnetometer, Nat. Commun. **14**, 5784 (2023).

[11] M. Bulatowicz, R. Griffith, M. Larsen, J. Mirijanian, C. B. Fu, E. Smith, W. M. Snow, H. Yan, and T. G. Walker, Laboratory search for a long-range T-odd, P-odd interaction from axionlike particles using dual-species nuclear magnetic resonance with polarized ^{129}Xe and ^{131}Xe gas, Phys. Rev. Lett. **111**, 102001 (2013).

[12] H. Su, Y. Wang, M. Jiang, W. Ji, P. Fadeev, D. Hu, X. Peng, and D. Budker, Search for exotic spin-dependent interactions with a spin-based amplifier, Sci. Adv. **7**, eabi9535 (2021).

[13] Y. Wang *et al.*, Limits on axions and axionlike particles within the axion window using a spin-based amplifier, Phys. Rev. Lett. **129**, 051801 (2022).

[14] Y. Wang *et al.*, Search for exotic parity-violation interactions with quantum spin amplifiers, Sci. Adv. **9**, eade0353 (2023).

[15] Y.-K. Feng, D.-H. Ning, S.-B. Zhang, Z.-T. Lu, and D. Sheng, Search for monopole-dipole interactions at the submillimeter range with a ^{129}Xe-^{131}Xe-Rb comagnetometer, Phys. Rev. Lett. **128**, 231803 (2022).

[16] D. F. J. Kimball, J. Dudley, Y. Li, D. Patel, and J. Valdez, Constraints on long-range spin-gravity and monopole-dipole couplings of the proton, Phys. Rev. D **96**, 075004 (2017).

[17] L. Hunter, J. Gordon, S. Peck, D. Ang, and J.-F. Lin, Using the Earth as a polarized electron source to search for long-range spin-spin interactions, Science **339**, 928 (2013).

[18] M. Rosenberry and T. Chupp, Atomic electric dipole moment measurement using spin exchange pumped masers of ^{129}Xe and ^{3}He, Phys. Rev. Lett. **86**, 22 (2001).

[19] W. Griffith, M. D. Swallows, T. H. Loftus, M. V. Romalis, B. R. Heckel, and E. N. Fortson, Improved limit on the permanent electric dipole moment of ^{199}Hg, Phys. Rev. Lett. **102**, 101601 (2009).

[20] N. Sachdeva *et al.*, New limit on the permanent electric dipole moment of ^{129}Xe using ^{3}He comagnetometry and squid detection, Phys. Rev. Lett. **123**, 143003 (2019).

[21] F. Allmendinger, I. Engin, W. Heil, S. Karpuk, H.-J. Krause, B. Niederländer, A. Offenhäusser, M. Repetto, U. Schmidt, and S. Zimmer, Measurement of the permanent electric dipole moment of the ^{129}Xe atom, Phys. Rev. A **100**, 022505 (2019).

[22] B. Venema, P. Majumder, S. Lamoreaux, B. Heckel, and E. Fortson, Search for a coupling of the Earth's gravitational field to nuclear spins in atomic mercury, Phys. Rev. Lett. **68**, 135 (1992).

[23] T. Wu, J. W. Blanchard, D. F. J. Kimball, M. Jiang, and D. Budker, Nuclear-spin comagnetometer based on a liquid of identical molecules, Phys. Rev. Lett. **121**, 023202 (2018).

[24] M. Ledbetter, S. Pustelny, D. Budker, M. V. Romalis, J. W. Blanchard, and A. Pines, Liquid-state nuclear spin comagnetometers, Phys. Rev. Lett. **108**, 243001 (2012).

[25] S.-B. Zhang, Z.-L. Ba, D.-H. Ning, N.-F. Zhai, Z.-T. Lu, and D. Sheng, Search for spin-dependent gravitational interactions at earth range, Phys. Rev. Lett. **130**, 201401 (2023).

[26] Z. Wang, X. Peng, R. Zhang, H. Luo, J. Li, Z. Xiong, S. Wang, and H. Guo, Single-species atomic comagnetometer based on ^{87}Rb atoms, Phys. Rev. Lett. **124**, 193002 (2020).

[27] F. Allmendinger *et al.*, W. Heil, S. Karpuk, W. Kilian, A. Scharth, U. Schmidt, A. Schnabel, Yu. Sobolev, and K. Tullney, New limit on Lorentz-invariance- and CPT-violating neutron spin interactions using a free-spin-precession ^{3}He ^{129}Xe comagnetometer, Phys. Rev. Lett. **112**, 110801 (2014).

[28] M. Smiciklas, J. Brown, L. Cheuk, S. Smullin, and M. V. Romalis, New test of local Lorentz invariance using a ^{21}Ne-Rb-K comagnetometer, Phys. Rev. Lett. **107**, 171604 (2011).

[29] J. Brown, S. Smullin, T. Kornack, and M. Romalis, New limit on Lorentz- and CPT-violating neutron spin interactions, Phys. Rev. Lett. **105**, 151604 (2010).

[30] W. Terrano and M. Romalis, Comagnetometer probes of dark matter and new physics, Quantum Sci. Technol. **7**, 014001 (2021).

[31] H. Dang, A. C. Maloof, and M. V. Romalis, Ultrahigh sensitivity magnetic field and magnetization measurements with an atomic magnetometer, Appl. Phys. Lett. **97**, 151110 (2010).

[32] I. Kominis, T. Kornack, J. Allred, and M. V. Romalis, A subfemtotesla multichannel atomic magnetometer, Nature (London) **422**, 596 (2003).

[33] C. Gemmel *et al.*, Ultra-sensitive magnetometry based on free precession of nuclear spins, Eur. Phys. J. D **57**, 303 (2010).

[34] M. Padniuk, M. Kopciuch, R. Cipolletti, A. Wickenbrock, D. Budker, and S. Pustelny, Response of atomic spin-based sensors to magnetic and nonmagnetic perturbations, Sci. Rep. **12**, 324 (2022).

[35] M. Limes, D. Sheng, and M. V. Romalis, ^{3}He-^{129}Xe comagnetometery using ^{87}Rb detection and decoupling, Phys. Rev. Lett. **120**, 033401 (2018).

[36] T. Sato *et al.*, Development of co-located ^{129}Xe and ^{131}Xe nuclear spin masers with external feedback scheme, Phys. Lett. A **8**, 588 (2018).

[37] P. Gomez, F. Martin, C. Mazzinghi, D. B. Orenes, S. Palacios, and M. W. Mitchell, Bose-Einstein condensate comagnetometer, Phys. Rev. Lett. **124**, 170401 (2020).

[38] T. Kornack and M. Romalis, Dynamics of two overlapping spin ensembles interacting by spin exchange, Phys. Rev. Lett. **89**, 253002 (2002).

[39] K. Wei *et al.*, Ultrasensitive atomic comagnetometer with enhanced nuclear spin coherence, Phys. Rev. Lett. **130**, 063201 (2023).

[40] W. Quan, K. Wei, T. Zhao, H. Li, and Y. Zhai, Synchronous measurement of inertial rotation and magnetic field using a K-Rb-^{21}Ne comagnetometer, Phys. Rev. A **100**, 012118 (2019).

[41] R. Li, W. Fan, L. Jiang, L. Duan, W. Quan, and J. Fang, Rotation sensing using a K-Rb-^{21}Ne comagnetometer, Phys. Rev. A **94**, 032109 (2016).

[42] T. G. Walker and W. Happer, Spin-exchange optical pumping of noble-gas nuclei, Rev. Mod. Phys. **69**, 629 (1997).

[43] T. R. Gentile, P. Nacher, B. Saam, and T. Walker, Optically polarized ^{3}He, Rev. Mod. Phys. **89**, 045004 (2017).

[44] See Supplemental Material at http://link.aps.org/supplemental/10.1103/PhysRevLett.133.023202 for details of experimental apparatus, calibration methods, derivation of self-compensation frequency and azimuth angle, Fano resonance,and quadrature detection method.

[45] R. Shaham, O. Katz, and O. Firstenberg, Strong coupling of alkali-metal spins to noble-gas spins with an hour-long coherence time, Nat. Phys. **18**, 506 (2022).

[46] A. E. Miroshnichenko, S. Flach, and Y. S. Kivshar, Fano resonances in nanoscale structures, Rev. Mod. Phys. **82**, 2257 (2010).

[47] A. Redfield and S. D. Kunz, Quadrature Fourier NMR detection: Simple multiplex for dual detection and discussion, J. Magn. Reson. **19**, 250 (1975).

[48] P. W. Graham and S. Rajendran, New observables for direct detection of axion dark matter, Phys. Rev. D **88**, 035023 (2013).

[49] K. Wei, Wei Ji, C. Fu, A. Wickenbrock, V. V. Flambaum, J. Fang, and D. Budker, Constraints on exotic spin-velocity-dependent interactions, Nat. Commun. **13**, 7387 (2022).

[50] W. Ji, Y. Chen, C. Fu, M. Ding, J. Fang, Z. Xiao, K. Wei, and H. Yan, New experimental limits on exotic spin-spin-velocity-dependent interactions by using $SmCo_5$ spin sources, Phys. Rev. Lett. **121**, 261803 (2018).

[51] T. Kornack, S. Smullin, S.-K. Lee, and M. Romalis, A low-noise ferrite magnetic shield, Appl. Phys. Lett. **90**, 223501 (2007).

[52] J.-H. Storm, P. Hömmen, D. Drung, and R. Körber, An ultra-sensitive and wideband magnetometer based on a superconducting quantum interference device, Appl. Phys. Lett. **110**, 072603 (2017).